Cement Hydration from Hours to a Century Controlled by Diffusion through Barrier Shells of C-S-H

Saeed Rahimi-Aghdam[a], Zdeněk P. Bažant[b,*], M.J. Abdolhosseini Qomi[c,]

[a] *Graduate Research Assistant, Northwestern University*
[b] *McCormick Institute Professor and W.P. Murphy Professor of Civil and Mechanical Engineering and Materials Science, Northwestern University*
[c] *Assistant Professor, University of California, Irvine*

Abstract

Although a few good models for cement hydration exist, they have some limitations. Some do not take into account the complete range of variation of pore relative humidity and temperature, and apply over durations limited from up a few months to up to about a year. The ones that are applicable for long durations are either computationally too intensive for use in finite element programs or predict the hydration to terminate after few months.However, recent tests of autogenous shrinkage and swelling in water imply that the hydration may continue, at decaying rate, for decades, provided that a not too low relative pore humidity (above 0.7) persists for a long time, as expected for the cores of a thick concrete structural members. Therefore, and because design lifetimes of over hundred years are required for large concrete structures, a new hydration model for a hundred year lifespan is developed. The new model considers that, after the first day of hydration, the remnants of anhydrous cement grains, gradually consumed by hydration, are enveloped by contiguous, gradually thickening, spherical barrier shells of calcium-silicate hydrate (C-S-H). The hydration progress is controlled by diffusion of water from capillary pores through the barrier shells toward the interface with anhydrous cement. The diffusion is driven by a difference of humidity, defined by equivalence with the difference in chemical potential

*Corresponding author. McCormick Institute Professor and W.P. Murphy Professor of Civil and Mechanical Engineering and Materials Science, Northwestern University, 2145 Sheridan Road, CEE/A135, Evanston, Illinois 60208

Email address: z-bazant@northwestern.edu (Zdeněk P. Bažant)

of water. Although, during the period of 4 to 24 hours, the C-S-H forms discontinuous nano-globules around the cement grain, an equivalent barrier shell control was formulated for this period, too, for ease and effectiveness of calculation. The entire model is calibrated and validated by published test data on the evolution of hydration degree and hydration heat for various cement types, particle size distributions, water-cement ratios and temperatures. Computationally, this model is sufficiently effective for calculating the evolution of hydration degree (or aging) at every integration point of every finite element in a large structure.

Keywords: Hydration, Diffusion Barrier, Humidity, Effective Permeability

---

1. Introduction

Bridges, super-tall buildings and other large concrete structures are supposed to be designed for lifetimes in excess of hundred years. However, much shorter lifetimes have often been experienced. This is documented by a Northwestern University database [1, 2] of 71 large-span prestressed bridges that developed seriously excessive deflections with concomitant damage. It was shown that the major cause was the design based on obsolete and inadequate prediction models for multi-decade creep [3, 4].

Although a significant progress toward developing a more realistic model has been made [5, 6], one aspect that needs a better mathematical model is the aging of concrete due to hydration. Since the creep is strongly affected by aging, and the aging is caused by solidification due to cement hydration, what is especially needed is a model that can predict the evolution of hydration for a hundred-year lifetime, and do so in a simple enough computationally effective way. To this end, we refine and extend the model presented in 2015 at ConCreep-10 see [7].

It is often thought that cement hydration is not a long-lived phenomenon. But that is true only if concrete dries up. In the cores of massive walls, high pore humidity may persist for decades even in structures exposed to dry environment. What makes the hydration process long-lived and progressively slower is that, after the first day, the anhydrous cement grains become enveloped in contiguous shells of cement hydrate. The shells are highly impermeable and allow only a very slow transport of water toward the anhydrous grain interface.

Therefore, the basic idea of the present model (whose outline was recently presented in ConCreep-10 proceedings [7]) is that the evolution of hydration is controlled by water diffusion through barrier shells of hydrated cement surrounding the anhydrous remnants of cement grains. Although contiguous barrier shells exist only after the first day of hydration, it will be convenient and computationally effective to introduce a hypothetical *equivalent* barrier shell model even for the first day.

The hydration of the cement is an extremely complex reaction involving chemo-physical phenomena on spanning from a nanometer to micrometers in length and from seconds to decades in time. Aside from creep, the hydration is a crucial process for heat generation, strength development, self desiccation and autogenous shrinkage. Developing a realistic model is essential for understanding and control of all these phenomena. The literature is large. The main works include, e.g., Jennings and Johnson [8]; Bentz and Garboczi [9]; Van Breugel [10] (whose model is known as HYMOSTRUC); Navi and Pignat [11]; Bentz [12] (whose model is known as CEMHYD3D); Maekawa et al. [13]; and Lin and Meyer [14].

Although some of the existing models are able to predict short- and mid-term hydration with sufficient accuracy, they consider either no physics or only the physical processes during the first few hours after mixing. Besides they are computationally too demanding for use in finite element programs for structural analysis. Also, the existing hydration models do not calculate the decrease of pore relative humidity caused by hydration, i.e., the self-desiccation, although this phenomenon is critical for understanding and modeling of autogenous shrinkage and drying creep, especially long-term [15, 16, 17, 18]. In older studies, the self-desiccation and autogenous shrinkage were generally ignored since they were negligible in old concretes with high water-cement ratios or no admixtures, or both. Recently, though, the trend toward high performance concretes raises the importance of the evolution of hydration for predicting the creep, shrinkage and self-desiccation, especially long-term.

Therefore, the present study aims to develop a new and complete hydration model. The goal is not only to predict the evolution of cement hydration with heat generation, but also to provide underpinning in the physics of hydration and achieve a model that would be credible for predicting century-long hydration with its effect on the pore humidity evolution. To this end, the model is based on the water transport through the aforementioned C-S-H barriers and conveniently considers the pore humidity (or

relative vapor pressure) as the driving force controlling the hydration rate. Simplicity, computational efficacy and usability in finite element program is also an important goal. Note that although in this study the water transport is considered to be the rate controlling process, there are also some other possible rate controlling processes including: 1- Ion diffusion, and 2- Slow down (even stop) of hydration reaction due to the effect of negative capillary pressure on cement dissolution rate [19]. Ion diffusion should be in balance with water transport since both should occur simultaneously to hydration reaction continues. Therefore, either of these processes could be considered as the main rate controlling process, but for simplicity the water transport has been chosen in this study. In addition, in order to consider the effect of capillary pressure on rate of reaction, the hydration reaction was considered to be stopped at high negative capillary tension (low relative humidity) as it was shown by Flat et al. (2011) [19].

The pore relative humidity (or just humidity) drives shrinkage, greatly influences creep and facilitates the alkali-silica reaction (ASR). As shown in Fig. 1, a humidity decrease results from both external drying and self-desiccation, the latter being caused by hydration. This figure illustrates how the two shrinkage driving forces interact. At drying exposure, the drying front spreads at a rapidly decaying rate into a slab, as described by a nonlinear diffusion equation [20]. For thick slabs, the core can remain unaffected by external drying for a very long time. This makes it clear that the self-desiccation, driven by hydration, can be the cause of a large pore humidity drop and play for a long time a significant role. These are situations where the evolution of hydration degree over months and years, even many decades, needs to be realistically modeled.

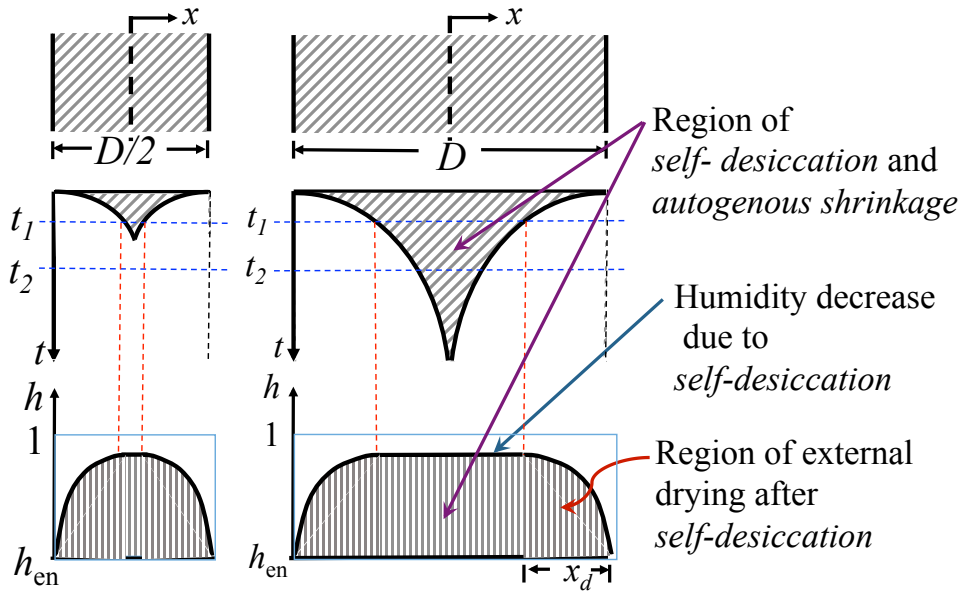

Figure 1: A schematic illustration of size effect in combined drying and self-desiccation causing autogenous shrinkage.

There are two recent observation that lead to the conclusion that the hydration and the consequent self-desiccation may be long-lived, proceeding at higher pore humidities (at decaying rate) for years, even decades (cf. Fig. 1 in [7]): Both the terminal autogenous shrinkage and the swelling under water immersion proceed logarithmically up to at least ten years. From this one may conclude that 1) The hydration, too, proceeds, at not too low humidity, for years, probably even decades, and 2) the hydration reaction on the micrometer level of cement paste may be expansive, even though on the nanolevel it is contractive, as known for more than a century [7]. The latter conclusion was explained by the crystal growth pressure of growing and contacting barrier shells of C-S-H, which is more than offset by contraction caused by a decrease of chemical potential of nanopore water related to increased capillary tension. This multi-year or multi-decade evolution cannot be described by the existing hydration models because either they predict the hydration to terminate within a few months and not more than a year or they are computationally too expensive to use in finite element program for such a long duration.

2. Qualitative Description of Cement Hydration

The ordinary portland cement (OPC) comprises various phases such as alite (C_3S), belite (C_2S), calcium aluminate (C_3A), tetracalcium aluminoferrite (C_4AF) and gypsum, as well as minor other phases (we use cement chemistry notation in which C, S, A and F stand, respectively, for CaO, SiO_2, Al_2O_3 and Fe_2O_3) [21]. C_3S and C_2S are two major components of OPC. The hydration mechanisms of OPC systems are extremely complex and involve chemo-physical phenomena whose scales span from nanometer to micrometers in length and from seconds to $\gg$ years in time. The hardened cement paste, as formed during the hydration process, is highly porous, with pore size distribution ranging from nanometers to millimeters. The cement paste's porosity, ϕ^p, may be divided into two components (excluding the interlayer porosity)[22]; $\phi^p = \phi^{gel} + \phi^{ip}$, where ϕ^{ip} and ϕ^{gel} are, respectively, inter-particle porosity (that often referred to as capillary porosity) and gel porosity. The inter-particle porosity represents the volume that originally exists between the anhydrous cement grains, part of which is gradually filled with the hydration products, the C-S-H gel and the portlandite. The gel porosity represents the pores that are exists inside the C-S-H gel. The gel porosity includes pores with various sizes and generally it has the characteristic dimension of 5.6 nm. The characteristic length scale in which Kelvin equation relates correctly the liquid meniscus curvature to pore vapor pressure, is approximately large than 3 nm. Therefore, the gel porosity includes some pores that Kelvin equation is valid for them ϕ^{Kp} and others in which Kelvin equation fails ϕ^{np}.

Due to the porous nature of C-S-H gel and a variable degree of saturation, the cement hydration is commonly regarded as a non-stoichiometric reaction. Here, we will consider only the part of the reaction that produces the solid C-S-H at the nano-level. The nano-level hydration reaction of C_2S and C_3S can be summarized as[23],

$$C_2S + 2.1H \rightarrow C_{1.7}SH_{1.8} + 0.3CH \tag{1a}$$

$$C_3S + 3.1H \rightarrow C_{1.7}SH_{1.8} + 1.3CH \tag{1b}$$

where $C_{1.7}SH_{1.8}$ and H are, respectively, the typical C-S-H type found in OPC pastes and water. The molecular water inside the nano-structure of C-S-H, usually referred to as inter-layer water or hindered adsorbed water layer, exhibits non-zero but very low mobility and diffusivity [24]. Therefore, we assume that the inter-layer water is part of the structure and does not

participate in the hydration process. The stoichiometric relations in Eq. 1 provide a means to calculate incremental evolution of different compounds in the reaction,

$$\mathrm{d}V_c = l_{\mathrm{C_{2,3}S}}\,[\mathrm{C_{2,3}S}] \tag{2a}$$

$$\mathrm{d}V_p = l_{\mathrm{CH}}\,[\mathrm{CH}] \tag{2b}$$

$$\mathrm{d}V_g^i = l_{\mathrm{CSH}}\,[\mathrm{CSH}] \tag{2c}$$

$$\mathrm{d}V_w = l_{\mathrm{H}}\,[\mathrm{H}] + \mathrm{d}V_g^i \phi^{np} + \mathrm{d}V_g^i \phi^{Kp} S^{Kp} \tag{2d}$$

where l_{M} and [M] are, respectively, the stoichiometry coefficient and the molar volume of compound M in Eq. 1. Table 1 gives the molar volume and density of the calcium-silicate phases present in the cement paste. We assume the porosity of C-S-H gel (gel porosity) to be 34% out of which for 30% Kelvin equation is assumed valid. The gel pores that kelvin equation is valid for them phi^{Kp} are considered not to be always saturated and S^{Kp} in Eq. 2d is the average saturation degree of these pores. We consider this saturation degree to be equal to the average saturation degree of inter-particle pores. It should be noted that, as it has been shown by some experiments [22, 25, 26] the density of C-S-H and thus its porosity is not constant. Due to simplicity and negligible effect on final results, the porosity of C-S-H is considered constant during calculating evolution of different compounds in the hydration reaction, but C-S-H densification and its porosity change is taken into account during the calculation of water transport through C-S-H by considering the C-S-H permeability as a function of its density.

Table 1: The molar volume and density of calcium-silicate phases present in the cement paste.

Phase	Molar volume (cm^3/mol)	Density(g/cm^3)
C_3S	72.5	3.15
C_2S	60	3.31
H_2O	18.1	1.0
C-S-H	110.1	2.05
CH	33.1	2.24

To study the evolution of hydration over time, it is imperative to express the consumption and production of different compounds in terms of water

consumption,

$$\zeta_{cw} = \frac{\mathrm{d}V_c}{\mathrm{d}V_w} \quad , \quad \zeta_{gw} = \frac{\mathrm{d}V_g}{\mathrm{d}V_w} \quad , \quad \zeta_{CHw} = \frac{\mathrm{d}V_p}{\mathrm{d}V_w} \tag{3}$$

where ζ_{mw} is the volume of the consumed or produced compound m per unit volume of consumed water. The rates of consumption of reactants and formation of hydration products depend strongly on the temperature at which the hydration occurs. To this end, the transition state theory presents a time rescaling relation that relates the time increment at temperature T, $\mathrm{d}t$, to the time increment at the reference temperature T_0, $\mathrm{d}t_0$, as follows,

$$\mathrm{d}t = \exp\left(-\frac{E_a}{R}\left(\frac{1}{T} - \frac{1}{T_0}\right)\right)\mathrm{d}t_0 \tag{4}$$

where T_0, E_a and R are, respectively, the reference temperature (293K), activation energy at the reference temperature, and universal gas constant.

3. Transport Through a Spherical C-S-H Shell

Fig. 2 illustrates the hydration reaction stages from setting time up to several years.

Because of complexity of the hydration reaction, simplifying assumptions are necessary. After an initial period Δt_1 of about 4 to 24 hours, a complete spherical barrier shell of C-S-H surrounding the remnant of anhydrous cement grain can exist, and is considered in the present analysis to persist for decades in duration. For simplicity, a fictitious 'equivalent shell' is here assumed to exist even during Δt_1, beginning with the time of set ($t = 0$).

In reality, the initial hydration, which is very fast, creates separate growing nano-scale globules of C-S-H clustered around the cement grain, which fuse at the end of Δt_1 into a continuous shell. Since the initial rate of hydration around the separate nano-globules is faster than predicted for the barrier shell, the inward diffusion of water through the shell toward the reaction interface of C-S-H with the remnant of anhydrous cement grain may initially (during Δt_1) be characterized by an increased effective hydraulic permeability, k_h. The gradual decrease of effective k_h as a function of the hydration degree reaches the actual permeability at the end of Δt_1 (see the next section, 4.

If a continuous barrier shell exists (hydration stages (d) and (e) in Fig. 2), the hydration kinetics is controlled by radial inward water diffusion through

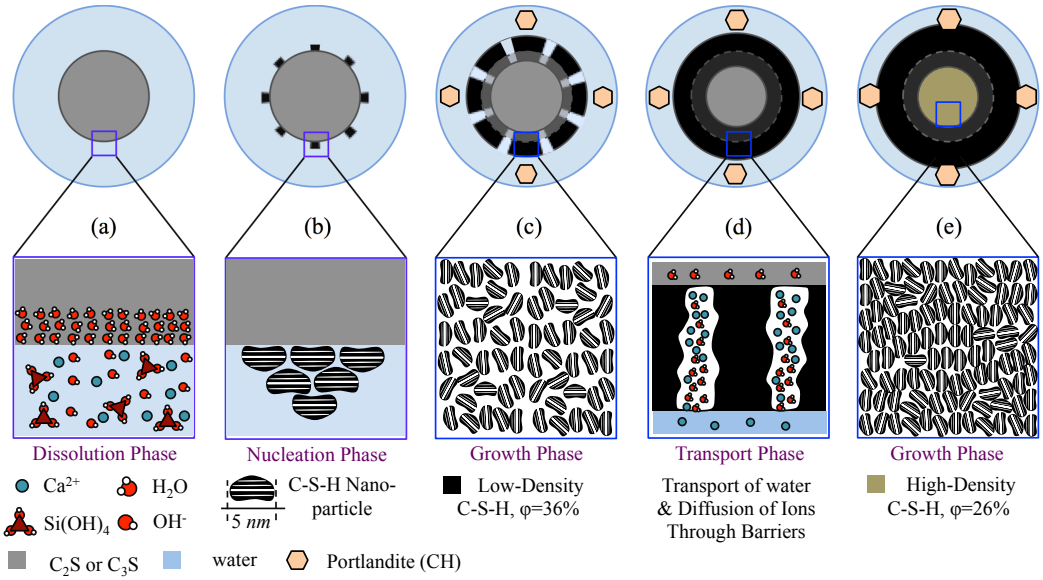

Figure 2: The schematics of a five-stage idealized thought model of cement hydration that combines transport and boundary nucleation growth mechanisms. (a) formation of a semi-impermeable layer around cement particles during the dormant period, (b) a symmetric nucleation of a constant number of C-S-H particles on the surface of cement particles, (c) an isotropic and self-similar growth of C-S-H nuclei with spatially constant but time varying growth rate, (d) overlapping of growing C-S-H nuclei and the coverage of the entire surface with hydrates which terminates the nucleation-growth process, (e) the uniform growth of C-S-H particles that is controlled chiefly by the inward transport of water and the outward diffusion of ions to the solution.

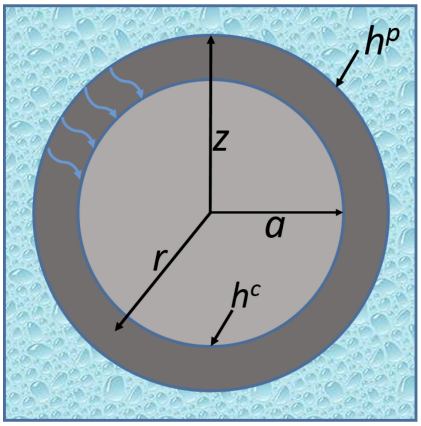

Figure 3: Transport through spherical shell

the porous C-S-H barrier, which is here assumed to occur uniformly over the shell. Let the shell thickness be $z - a$, where a is the decreasing radius of anhydrous cement grain particle and z is the growing outer radius of the shell surface (Fig. 3). Assuming spherical symmetry, the velocity of the inward radial diffusion of water may be assumed to follow the Darcy law:

$$v_w(r) = k_h \frac{\mathrm{d}p_v}{\mathrm{d}r} \tag{5}$$

where r = radial coordinate and k_h = hydraulic permeability (also called conductivity or filtration coefficient). The hydraulic conductivity can be written as,

$$k_h(T) = \frac{k_0}{\eta(T)} \tag{6}$$

where k_0 is the intrinsic permeability of porous medium and $\eta(T)$ = shear viscosity of water. The viscosity and thus the k_h depend on the reaction temperature that for simplicity this effect has considered using effective time Eq. 4.

It is instructive to express the aforementioned transport formulation in terms of the pore relative humidity h (often called 'humidity', for the sake of brevity);

$$h \;=\; \frac{p_v}{p_{sat}} \tag{7}$$

where p_v = partial pressure of water vapor and p_{sat} = saturation vapor pressure, which greatly increases with T. Although, fundamentally, the diffusion

of water through the shell is driven by the gradient of chemical potential of pore water, μ, it will be convenient to replace μ with the equivalent humidity h, even though water vapor exists neither in the C-H-S shell nor at the interface with the anhydrous cement. So we define:

$$h \;=\; e^{(\mu_0 - \mu M/RT)} \tag{8}$$

where μ_0 = chemical potential of water at saturation, and M = molecular weight of water = 18.02 g/mol. Inside the C-S-H shell, μ is the chemical potential of the adsorbed water (free or hindered) in the nanopores. Eq. 5 now takes the form:

$$v_w = B\frac{dh}{dr}\ , \quad B = \frac{k_0 p_{sat}}{\eta} \tag{9}$$

where B is the effective permeability (dimension m^2/s). Based on assuming incompressibility of diffusing water, the radial discharge, Q_w, or volume flow rate, is uniform for all radial directions and is

$$Q_w = A(r)v_w(r) = 4\pi r^2 B\frac{\mathrm{d}h(r)}{\mathrm{d}r} \tag{10}$$

which is a first-order ordinary differential equation. Its solution reads,

$$h(r) = \frac{-Q_w}{4\pi r B} + C \tag{11}$$

where C is the integration constant, which can be determined from the boundary conditions.

The first boundary condition at the interface $r = a$ of C-S-H with the remnant of anhydrous cement grain is,

$$h(a) = h_c \tag{12}$$

where h_c is the equivalent humidity at the interface of C-S-H shell with the anhydrous cement. As an approximation, probably a good one, we may consider that $h_c = 0.75$ for $T = 20°C$, which is believed to be the humidity below which the hydration reaction does not proceed. Note that this value of h_c might be different for concretes with some special admixtures, such as the silica fume (SF); see Bouny[27] who showed in 1999 that, for SF, h_c can be as low as 0.60).

The second boundary condition, at $r = z$, is $h(z) = h_p$ = pore relative humidity. Substituting both boundary conditions into Eq. 11, we get:

$$Q_w = 4\pi a B \, \frac{\langle h_p - h_c \rangle}{1 - \dfrac{a}{z}} \ , \qquad C = \frac{h_p - h_c \dfrac{a}{z}}{1 - \dfrac{a}{z}} \tag{13}$$

where $\langle x \rangle = \max(x, 0)$ serves to give $Q_w = 0$ when $h_p < h_c$. Then, inserting this into Eq. 11, we obtain the relative humidity profile in terms of dimensionless quantities:

$$h\,(r) = \frac{\left(\dfrac{r}{a} h_p - \dfrac{r}{z} h_c\right) - (\langle h_p - h_c \rangle)}{\left(\dfrac{r}{a} - \dfrac{r}{z}\right)} \tag{14}$$

4. Effective Permeability Model

In the initial hydration period of one day or less, two stages of different kinetics can be distinguished (for a comprehensive discussion, see, e.g., [28]). The first stage is a short 'dormant' period right after the time of set, having the duration of a few hours. Second comes the stage of nucleation and growth of nano-globules of C-S-H. They are necessarily disconnected. The reason: since the C-S-H molecules have an effective diameter of 5 to 50 nm, a continuous shell, obviously, cannot form until the volume of all the C-S-H globules becomes sufficient to fill a continuous shell of that same thickness (Fig 4). The hydration degree α at which this occurs is called the critical hydration degree, α_c. It is typically attained within the first day (in Sec. 5, an empirical equation for α_c will be proposed). For $\alpha > \alpha_c$, a continuous barrier shell of C-S-H exists and grows.

The initial behavior just described obviously cannot be predicted with the radial spherical transport of water. Nevertheless, the permeability in this model can be adjusted and calibrated as a function of the hydration degree α_c, so as to match the volume growth of the nano-globules. In other words, instead of modeling the two initial hydration stages in detail, we consider an *equivalent* fictitious barrier giving the same radial water flux and the same growth of α as the nano-globule growth.

Based on the one-dimensional transport model in Eq. 13, the water discharge for one cement particle is,

$$Q_t^1 = 4\pi a_t z_t B_{eff}(\alpha, h_p) \frac{h_p - h_c}{z_t - a_t} \tag{15}$$

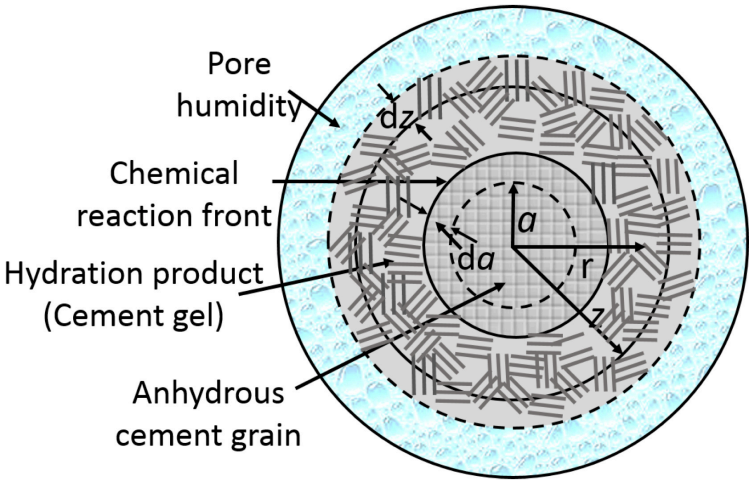

Figure 4: A schematic representation of spherical (homogeneous) hydration.

where, for brevity, $z_t = z(t)$, $a_t = a(t)$, and B_{eff} = effective permeability, which is a function of the hydration degree and the inter-particle pore humidity. Assuming both functions to be independent, we can write,

$$B_{eff} = B_0 f_0(h_p) f_4(\alpha) \tag{16}$$

where B_0 is an unknown constant. In the present simulations we consider $B_0 = 1.0 \cdot 10^{-11}\text{m}^2/\text{day}$ for alite specimens and $B_0 = 7.32 \cdot 10^{-12}\text{m}^2/\text{day}$ for cement specimens.

Function $f_4(\alpha)$ describes the dependence of B on the hydration degree, and is assumed as follows:

$$f_4(\alpha) \;=\; \gamma\, e^{-\gamma}, \quad \gamma = \left(\frac{\alpha}{\alpha_{max}}\right)^m \quad \text{for} \quad \alpha \le \alpha^* \tag{17a}$$

$$f_4(\alpha) \;=\; (\beta/\alpha_s)^m e^{(\beta/\alpha_c)^m}, \quad \beta = \alpha - \alpha^* + \alpha^* \alpha_s/\alpha_{max} \quad \text{for} \quad \alpha > \alpha^* \tag{17b}$$

Here α_{max} = hydration degree at which the permeability reaches its maximum, and $\alpha_{max} = \alpha_c/2$ where α_c is the critical hydration degree, defined here as the hydration degree at which the C-S-H barrier around the cement particle gets completed (typically about 24 hours). Constants α^*, m and α_s are empirical and are considered as $\alpha^* = 1.5\alpha_{max}$, $m = 2$ for alite samples and $m = 1.8$ for cement samples, and $\alpha_s = 0.3$. Note that $\alpha - \alpha^* + \alpha^* \alpha_s/\alpha_{max}$ is used in Eq. 17b instead of α, for f_4 to be continuous.

The expression for $f_4(\alpha)$ gives an increasing water discharge rate until the hydration degree reaches α_{max}, and a decreasing rate afterwards. The start of $f_4(\alpha)$ from a small value can be explained by the metastable barrier hypothesis [29, 30, 31, 32, 33, 28] or the slow dissolution step hypothesis [34, 35, 36, 37, 38, 28]. The gradual decrease of $f_4(\alpha)$ after α_{max} is explained by the filling of capillary pores with hydration products [39, 40]. It should be noted that the considered permeability function is in agreement with recent NMR results by Knigsberger et al. [Kon16] for evolution of C-S-H density and porous structure. These recent NMR data, show the density of C-S-H initially decreases up to α_{max} and later the density increases. This is exactly the same kind of behavior that has considered here for permeability of C-S-H barrier.

Now that we can calculate the total water discharge, we need to analyze the evolution of hydration degree and pore humidity change. For the sake of simplicity, we express the volume of each component or phase as a fraction of unit volume of concrete; so, V^w, V^c, V^a are the volumes of water, cement and aggregate per unit volume of concrete and are dimensionless numbers such that

$$V_0^w + V_0^c + V_0^a = 1 \ (\mathrm{m}^3/\mathrm{m}^3), \qquad \frac{V_0^w \rho_w}{V_0^c \rho_c} = w/c, \qquad \frac{V_0^a \rho_a}{V_0^c \rho_c} = a/c \tag{18}$$

where $w/c, a/c =$ water-cement and aggregate-cement ratios (by weight); ρ_w, ρ_c and ρ_a are, respectively, the specific mass of water (1000 kg/m^3), cement (here considered as 3150 kg/m^3), and aggregates (here 1600 kg/m^3) for gravel and sand combined). The corresponding relative volumes are

$$V_0^c = \frac{\rho_a \rho_w}{\rho_a \rho_w + \rho_c \rho_w a/c + \rho_c \rho_a} w/c \tag{19a}$$

$$V_0^a = \frac{\rho_c \rho_w a/c}{\rho_a \rho_w + \rho_c \rho_w a/c + \rho_c \rho_a} w/c \tag{19b}$$

$$V_0^w = \frac{\rho_a \rho_c w/c}{\rho_a \rho_w + \rho_c \rho_w a/c + \rho_c \rho_a w/c} \tag{19c}$$

The number of cement particles, n_g, per unit volume of cement, is obtained from the volume of cement and the particle size, a_0:

$$n_g = \frac{V_0^c}{\frac{4}{3}\pi a_0^3} \tag{20}$$

The initial volumes of different phases at the time of set may be expressed as

$$V_{set}^{c} = (1 - \alpha_{set})V_0^c \qquad V_{set}^{CH} = \zeta_{CHc}\alpha_{set}V_0^c \qquad V_{set}^{g} = \zeta_{gc}\alpha_{set}V_0^c \tag{21}$$

where α_{set} = hydration degree at the time of set, which is approximately related to the end of the dormant period; ζ_{CHc} = volume of portlandite per unit volume of consumed cement; $\zeta_{CHc} = \zeta_{CHw}/\zeta_{cw}$ where the ζ_{gc} value is the same as it is for the C-S-H gel, i.e., $\zeta_{gc} = \zeta_{gw}/\zeta_{cw}$. At the time of set, the radius of cement particles a_{set} and radius of C-S-H barrier z_{set} may be calculated as,

$$a_{set} = \left(\frac{V_{set}^{c}}{\frac{4}{3}\pi n_g}\right)^{\frac{1}{3}}, \qquad z_{set} = \left(\frac{V_{set}^{c} + V_{set}^{g}}{\frac{4}{3}\pi n_g}\right)^{\frac{1}{3}} \tag{22}$$

Having all the necessary parameters at hand for the time of set, we calculate finite increments to track the evolution of state variables throughout the hydration process. The incremental, $\mathrm{d}V^g$, and total, $V^g_{t+\mathrm{d}t}$, volumes of C-S-H gel produced during $\mathrm{d}t$ can be calculated as,

$$V^{c}_{t+\mathrm{d}t} = V_t^c + \mathrm{d}V_t^c = V_t^c - n_g Q_t^1 \zeta_{cw}\mathrm{d}t \tag{23a}$$

$$V^{g}_{t+\mathrm{d}t} = V_t^g + \mathrm{d}V_t^g = V_t^g + n_g Q_t^1 \zeta_{gw}\mathrm{d}t \tag{23b}$$

$$V^{CH}_{t+\mathrm{d}t} = V_t^{CH} + \mathrm{d}V_t^{CH} = V_t^{CH} + n_g Q_t^1 \zeta_{CHw}\mathrm{d}t \tag{23c}$$

where $V_t = V(t)$, etc., and ζ_{cw}, ζ_{gw} and ζ_{CHw} are, respectively, the volumes of the cement consumed, the C-S-H gel produced and the portlandite per unit volume of discharged water, all defined in Sec. 2.

The radius and the hydration degree of the cement particles can be updated from the amount of reacted cement, dV_t^c;

$$a_{t+\mathrm{d}t} = a_t + \mathrm{d}a_t = a_t + \frac{1}{4\pi a_0^2 n_g}\mathrm{d}V_t^c \tag{24a}$$

$$\alpha_{t+\mathrm{d}t} = \alpha_t + \mathrm{d}\alpha_t = \alpha_t - \frac{3}{4\pi a_0^3 n_g}\mathrm{d}V_t^c \tag{24b}$$

Although a sparse solid framework with very limited continuity develops already at the time of set, it is at first so sparse that most C-S-H barriers surrounding cement particles are too thin to contact each other. Soon, however, more barrier shells touch and later, as the number of contacting shells

and their contact areas grow, the ratio of overall free shell surface relative to the radius diminishes.

Let $\hat{z}$ be the radius of contact-free shells giving the same free surface area as the actual shell radius z would if the shell surfaces were free. Exact calculation of $\hat{z}$ would be complicated but a good approximate formula can be obtained by asymptotic matching because the opposite asymptotic conditions are clear and simple:

1) $\hat{z} = z$ and $\mathrm{d}\hat{z}/\mathrm{d}z = 1$ for $z = a_0$, and

2) $\mathrm{d}\hat{z}/\mathrm{d}z = 0$ for big z. These asymptotic conditions can be most simply satisfied by the function:

$$\hat{z}^2 = \frac{z^2}{1 + \left(\frac{z-a_0}{u}\right)^2} \tag{25}$$

where u = constant that we may set it $a_0/2$. Note that the growth of z is theoretically limited by two finite bounds: 1) For low enough w/c and large enough cement grains, z could in theory reach the value of z_{max} for which the volume of all the spherical cement grains with barrier shells per unit volume of cement paste (without discounting shell overlaps) would be equal to all the pore space within the unit volume, i.e.,

$$z_{max}^2 = (1 - V_a)\,\frac{a}{4\pi n_g} \tag{26}$$

where n_g = number of cement grains with barrier shells per unit volume, and V_a = volume fraction of all aggregates. 2) For small enough cement grains and large enough w/c, the cement could hydrate completely, with no anhydrous cement left. In that case,

$$z_{max}^3 = V_0^c \zeta_{gc} \frac{3}{4\pi n_g} \tag{27}$$

where V_0^c = initial volume fraction of anhydrous cement and $\zeta_{gc} = \zeta_{gw}/\zeta_{cw}$ = volume of C-S-H gel produced per unit volume of cements. One could adjust Eq. 25 to conform to these theoretical bounds. But it is not necessary because: 1) when the volume of all the grains with barrier shells equals the original pore space, the present model indicates no water to remain and thus the hydration, with the growth of $\hat{z}$, to stop, and 2) the model also indicates the hydration to stop when all the cement gets hydrated.

If $\hat{z}$ is known, the increment of radius z during time step $(t, t+\mathrm{d}t)$ may be calculated as,

$$\mathrm{d}z_t = \frac{\mathrm{d}V_t^g + \mathrm{d}V_t^c}{4\pi\hat{z}^2} \quad \text{for} \;\; \alpha_t > \alpha_c \tag{28}$$

At this stage the only unknown parameter is the inter-particle pore humidity at the end of each time step, $h^p_{t+\mathrm{d}t}$. To find the humidity changes in inter-particle capillary porosity, we rely on the increment of saturation degree, S^{ip}. To relate the saturation degree to the relative humidity, we use the desorption isotherm. To this end, we begin with calculating the total inter-particle water content, V^w_{ip}, and its increment. Noting that the increment of V^w_{ip} should be equal to the incremental total water that diffuses through C-S-H gel, we have

$$V^w_{ip} = \phi^{ip} S^{ip}, \quad \mathrm{d}V^w_{ip} = \mathrm{d}\phi^{ip}_t S^{ip}_t + \phi^{ip}_t \mathrm{d}S^{ip}_t = -n_g Q^1_t \mathrm{d}t \tag{29}$$

The *desorption isotherm*, which relates the water saturation degree to the pore relative humidity, may be written as,

$$(1-h_p) = K_h(1-S^{ip}), \quad \mathrm{d}h_p = K_h \mathrm{d}S^{ip}_t \tag{30}$$

where K_h is the isotherm slope. The slope depends highly on the water-cement ratio, curing conditions and hydration degree of the cement paste. Here we limit attention to humidity levels higher than 75% and assume the isotherm slope to be constant, i.e., $K_h(w/c) = 1.2 - w/c$. Combining eqs. 29 and 30, we derive the humidity increment,

$$dh^p_t = K_h \left(\frac{-n_g Q^1_t \mathrm{d}t - \mathrm{d}\phi^{ip}_t S^{ip}_t}{\phi^{ip}_t} \right) \tag{31}$$

where $\mathrm{d}\phi^{ip}_t$ is the inter-particle porosity increment (a decrement) calculated as

$$\mathrm{d}\phi^{ip}_t = -(\mathrm{d}V^g_t + \mathrm{d}V^{CH}_t + \mathrm{d}V^c_t) \tag{32}$$

To evaluate Eq. 2d and subsequently the volumetric ratios in Eq. 3, we need the saturation degree of capillary pores, S^{cw}. For simplicity, we consider the saturation degree to be the average of the saturation degree in inter-particle pores and the saturation degree at the cement-gel interface, h_c, which we take as 0.75 because we assume that this is the equivalent humidity below which the hydration cannot proceed. In other words, hydration of

cement in contact with water proceeds rapidly, almost immediately, until the chemical potential of water cannot overcome the activation energy barrier as it drops below the value corresponding to 0.75.

So far, we have not yet considered the variation of permeability during hydration. Previous studies have indicated that a decrease of humidity strongly reduces the permeability of cement paste [20]. We model this effect by function f_0 in Eq. 16. Using Bažant and Najjar's equation [20], we may define f_0 as

$$f_0 = c_f + \frac{1 - c_f}{1 + \left(\frac{1-h_t^p}{1-h^*}\right)^{n_h}} \tag{33}$$

where h^*, n_h, c_f are empirical parameters and f_0 is the functional form. In this study, we set $n_h = 8$, $h^* = 0.85$ and $c_f = 0$.

Our analysis up to now up implied all of cement particles to have the same size. In reality, each cement has its own particle size distribution (PSD). This poly-dispersity may approximately be taken into account by defining the effective cement particle size as the size for which the same degree of hydration is reached as in the poly-disperse cement. Such an approximation is, in fact, necessary for our analysis since the particle size distributions of cements are usually unavailable for experimental data in literature. Since hydration is a surface-driven reaction, it is rational to consider the effective size as the size that keeps the total surface area constant. Therefore, in order to calculate the effective cement particle size, $D_{eff} = 2a_{eff}$, we first calculate the total surface area of all cement particles, A^{tot}. If we have a mono-disperse cement with radius a, the total surface area is,

$$A^{tot} = \frac{V^c}{\frac{4}{3}\pi a^3}(4\pi a^2) = \frac{3V^c}{a} \tag{34}$$

Thus, for poly-disperse cement with volume probability distribution function Γ, we have,

$$A^{tot} = \int_{V^c} \frac{3dV^c(a)}{a} = \int_a \frac{3\Gamma(a)da}{a} \tag{35}$$

Considering the effective size as the size that keeps the total surface area constant, we have

$$A^{tot} = \int_a \frac{3\Gamma(a)da}{a} = \frac{3V^c}{a_{eff}} = \frac{3\int_a \Gamma(a)da}{a_{eff}} \ , \ \ \rightarrow a_{eff} = \frac{\int_a \Gamma(a)da}{\int_a [\Gamma(a)/a]\mathrm{d}a} \tag{36}$$

where a_{eff} is the effective particle size in terms of the volume probability distribution function.

5. Hydration of Mono-Disperse Systems at Different Conditions

The critical hydration degree of cement paste, α_c, as defined earlier, is the hydration degree at which the C-S-H barrier shell becomes contiguous and complete. The value of α_c was shown by Bullard et al. [41] to be almost equal to the hydration degree at the end of first day. This value is strongly affected by the parameters of cement and concrete and the environmental conditions. It depends on various parameters, including the particle size distribution, water-cement ratio and temperature. These control parameters affect the structure of the nano- and capillary pore networks, as well as the reaction rate. Lacking quantitative experimental or theoretical models for the effects of these control parameters, we propose empirical equations, to be validated later, and assume the effects of these parameters to be independent, as follows:

$$\alpha_c = \alpha_c^0 f_1(a) f_2(w/c) f_3(T) \tag{37}$$

where α_c^0 is the calibration constant and f_1, f_2 and f_3 are empirical functions.

Assuming that the thickness of C-S-H gel, d_c, forming around the cement particle at the critical hydration degree is independent of particle size, we can introduce the approximation:

$$4\pi a^2 d_c \approx \frac{4}{3}\pi a^3 \alpha_c \ , \quad \alpha_c \propto \frac{d_c}{a} \quad \rightarrow \quad f_1(a) = \frac{a_0}{a} \tag{38}$$

Here a_0 is the reference radius, which is assumed as 6.5μm when there is no further information about the cement's particle size distribution. The last approximation is probably crude. A more accurate formulation to derive α_c is:

$$\frac{1}{1-\alpha_c} = \left(1 + \frac{d_c}{a(1-\alpha_c)^{\frac{1}{3}}}\right)^3 \tag{39}$$

but in this case we cannot find a closed-form expression for f_1 since the last formulation is nonlinear.

To consider the effect of water content ratio, we assume a linear function:

$$\alpha_c = \alpha_c^0 + m_c(w/c - 0.4) \quad \rightarrow \quad f_2(w/c) = 1 + \frac{m_c}{\alpha_c^0}(w/c - 0.4) \tag{40}$$

where α_c^0 = critical hydration degree at $w/c = 0.4$ and $m_c = 1.2$ = slope that is obtained by fitting the model to measured data on hydration at different w/c.

Similar to eqs. 4, we assume that α_c follows Arrhenius law:

$$f_3(T) = \exp\left[\frac{E_\alpha}{R}\left(\frac{1}{273+T_0} - \frac{1}{273+T}\right)\right] \tag{41}$$

where E_α is an activation energy. Data fitting gave the value $E_\alpha/R = 800$. We also constrain the critical hydration degree to be less than 0.65. For simplicity, we consider a direct relation between α_c and the hydration degree α_{set} at the time of set:

$$\frac{\alpha_{set}}{\alpha^0_{set}} = \frac{\alpha_c}{\alpha^0_c} \tag{42}$$

Here α^0_{set} is the hydration degree at time of set when the critical hydration degree is α^0_c.

6. Predicted Hydration Curves

Now we use the proposed method to predict the hydration curves under different control parameters. Fig. 5 presents the effect of particle size distribution on the hydration degree and the rate of the heat of hydration for alite systems with the mean particle sizes of 13, 18, 38 and 82μm which, respectively, correspond to effective particle sizes of 12, 17, 34 and 60μm. We calibrate the model for the 13 μm particle size only, and the rest are predictions.

The calibration parameters are $\alpha_0 = 0.011$ and $\alpha_{max} = 0.21$ and the time of set was considered as 2 hours. Fig. 6 shows the effect of water-cement ratio on the hydration degree of OPC pastes. For the tests of Danielson [43] (Fig. 6a), the effective permeability model is calibrated to $w/c = 0.3$, and the calibration parameters are $\alpha_0 = 0.07$ and $\alpha_{max} = 0.21$. For the tests of Bentz [44] (Fig. 6b), the model is calibrated for $w/c = 0.35$ and $\alpha_0 = 0.06$ and $\alpha_{max} = 0.26$.

Fig. 7 shows the effects of hydration temperature and cement type on the hydration degree. The activation energy and effective particle sizes for cements of Type I to Type III in Fig. 7.a-c are, respectively, $4.5{*}10^4$, $4.5{*}10^4$ and $5.0 * 10^4$J/mol and 12.5, 14 and 9μm [14]. The calibration parameters for Type I cement with $T = 24°$C are $\alpha_0 = 0.07$ and $\alpha_{max} = 0.24$. All the other results are predicted. Note that, through all the simulations, the Blaine fineness of cement equal to 350m^2/kg was considered to correspond to particle size 13μm.

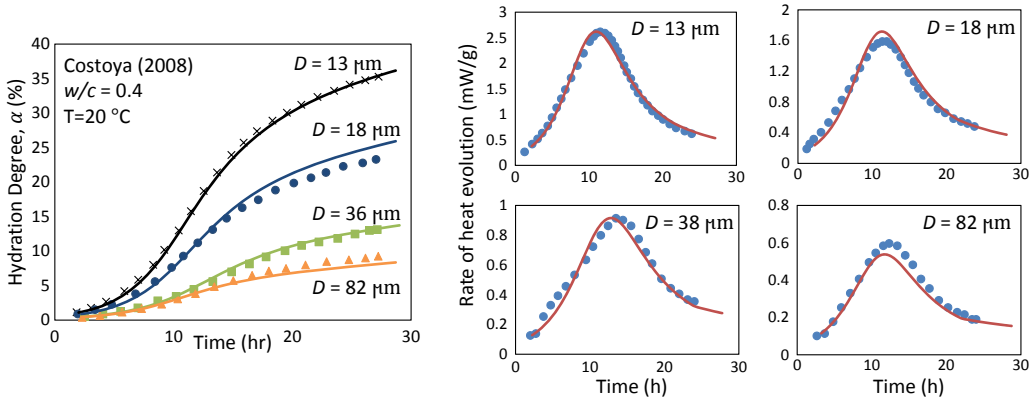

Figure 5: Examining the predictive power of the effective permeability model vs. experimental measurements of Costoya [42] on alite phase. a) Hydration degree, b-e) The rate of heat of hydration for different particle sizes.

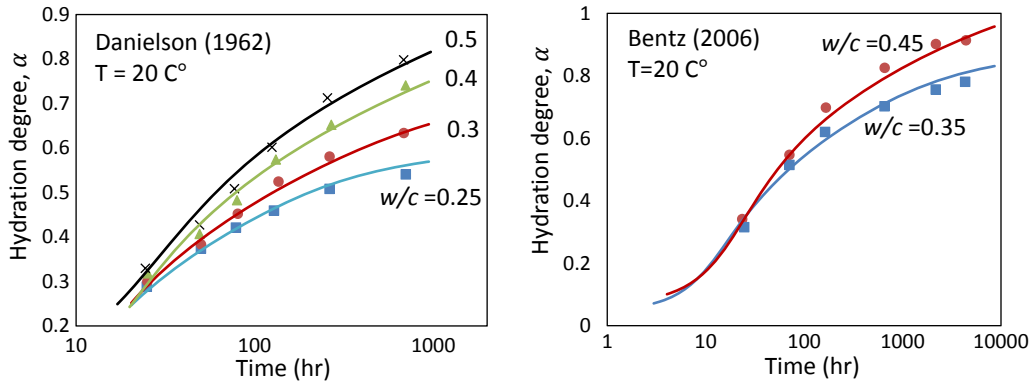

Figure 6: Prediction of the hydration degree of OPC for different water-to-cement ratios using effective permeability model against experimental measurement of a) Danielson [43] and b) Bentz [44].

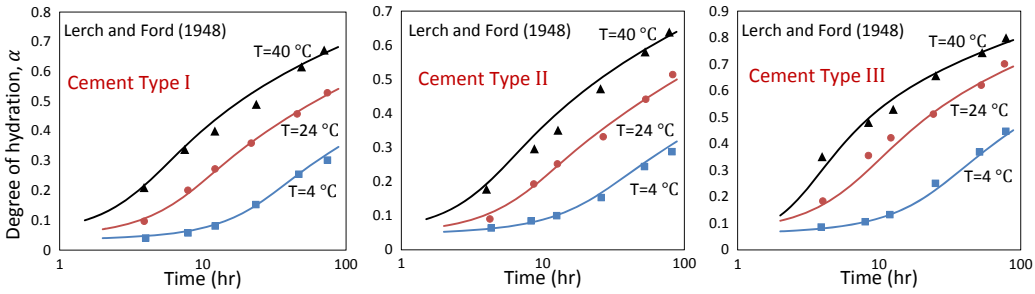

Figure 7: Prediction of the hydration degree of different cement types at different temperatures against experimental measurements of Lerch and Ford [45]. a) cement type-I, b) cement type-II and cement type-III.

For normal cement paste the permeability of C-S-H shell barrier is ranged approximately from 10^{-23} to 10^{-25} m^2. This permeability change is due to change of porosity of C-S-H gel [22, 26, 25]. These values for permeability are smaller than the one that reported by Power and Brownyard [39] ($7x10^{-23}$ m^2) for dense cement paste. Having lower value of permeability for C-S-H shell barrier than whole cement gel can be explained by the fact that in the transport through the C-S-H shell barrier case, the water should transport through whole C-S-H barrier that includes gel with various densities. Especially, the C-S-H shell barrier may include some dense and ordered C-S-H gel with very low permeability that water should transport through them as well, while in transport through cement paste case, water may mostly transport through less dense part and choose the path with higher permeability. Furthermore, in transport through barrier case, the relative humidity has significant effect on having lower permeability since near the anhydrous cement the relative humidity is lower and thus as it has shown in Bazant-Najjar [20] model the permeability may be significantly lower (some order). On the other hand, for whole cement gel case water may flow majorly through a path that includes gel with higher relative humidity and thus higher permeability.

Finally note that a_{eff} is different from the average particle size, a_m. These two should not be used interchangeably. Here we use the effective size rather than the average size. For further illustration, we use a set of poly-disperse alite systems with the volume probability distribution function given in Fig. 8.(a). First we calibrate the present effective permeability model with an alite system in which the average and effective particle sizes are almost identical, calibration parameters are the same with other Costoya's experiments.

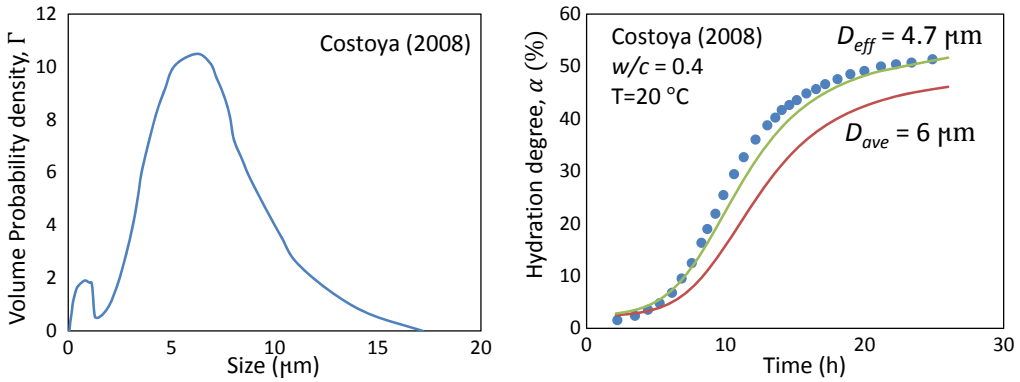

Figure 8: Effective particle size method. a) The volume probability distribution function of am elite system measured by Costoya [42]. b) Calculating the hydration degree using effective permeability model with both the average size (solid blue) and the effective size (solid red) and their comparison with experiment [42].

Subsequently we use these parameters to predict the hydration degree of the aforementioned alite system (see Fig. 8). Clearly the model with the average particle size deviates from the experimental data while the model with the effective particle size fits these data perfectly.

7. Humidity decrease due to self-desiccation

As just demonstrated, the present simplified model can quantitatively explain the hydration degree and its rate under different control parameters. But, as stated in Sec. 1, the main purpose is to predict, from these parameters, the shrinkage and swelling. This requires a realistic prediction of the evolution of humidity profiles throughout the lifetime.

Fig. 9 presents the humidity decrease due to self-desiccation as predicted by the present effective hydration model, compared to the experiments of Jiang et al. [46], for different water-cement ratios. At low water-cement ratio ($w/c = 0.25$), the simulated results are in good agreement with the experiments. However, this is not the case for high water-cement ratios, especially at the early age.

The underlying reason for this discrepancy can be our simplifying assumption that the desorption isotherm slope, K_h, remains constant during hydration. In fact, as the pore network evolves during hydration, K_h varies over time. Although the discrepancy is here not too significant, it could

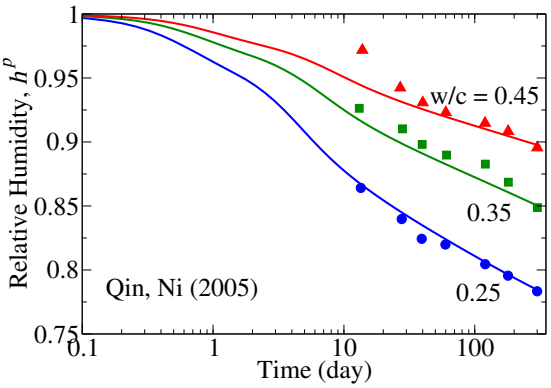

Figure 9: Humidity decrease due to self-desiccation at different water-to-cement ratios.

be significant in calculating the shrinkage of concretes with significant self-desiccation.

8. Algorithm for Calculation Hydration degree and Humidity Evolution

1. For the cement paste or concrete with known water-cement w/c and aggregate-cement a/c ratios, calculate the initial volume fraction of cement V_0^c and water V_0^w using Eq. 19.
2. calculate the average cement particle size (particle radius) a_0 based on the cement type. In this study, the Blaine fineness of cement equal to $350\text{m}^2/\text{kg}$ was considered to correspond to particle radius 6.5μm. Also, knowing V_0^c and a_0 calculate the number of cement particles, n_g, per unit volume of cement using Eq. 20.
3. Based on sample w/c and temperature T and average cement particle size a_0, choose a reasonable hydration degree for setting time α_{set} and the time that C-S-H barrier will be completed $alpha_c$ (Critical Hydration degree). For normal cement with $a_0 = 6.5\mu$m, $w/c = 0.4$ at $T = 20C°$C, $\alpha_{set} = 0.07$ and $\alpha_{set} = 0.3$ are good approximations. For samples with different T, w/c and cement type the reasonable value can be calculated using Eq. 37 to 42. In addition, the sample can be considered saturated at setting time ($h = 1$, $S^{ip} = 1$).
4. Knowing α_{set}, V_0^c calculate the volume fraction of cement V_{set}^c, portlandite V_{set}^{CH} and gel (C-S-H plus ettrengite) V_{set}^g Using Eq. 21, and having these volume fractions calculate the radius of cement particle

a_{set} and the radius of C-S-H barrier z_{set} using Eq. 22. Considering hydration chemical reaction, the following volume ratios may be used: $\zeta_{gc} = 1.52$, $\zeta_{CHc} = 0.59$ and $\zeta_{wc0} = 1.21$. It should be noted that ζ_{wc} can decrease from 1.21 to 1.15 as a function of saturation degree, but considering it as a constant value also can end up acceptable results.

5. At each time step, using hydration degree α and humidity h from previous step, calculate the water permeability B_{eff} using Eqs. 16, 17 and 33.
6. At each time step, using humidity h, cement particle size a and C-S-H barrier size z from previous time step plus calculated permeability, calculate the water discharge Q_t^1 using Eq. 15.
7. At each step using calculated water discharge Q_t^1, using Eq. 23 calculate the volume increment of cement $\mathrm{d}V_t^c$, portlandite $\mathrm{d}V_t^{CH}$ and gel $\mathrm{d}V_t^g$.
8. At each time step use the calculated $\mathrm{d}V_t^c$ to calculate the increment of hydration degree $\mathrm{d}\alpha_t$ cement particle radius $\mathrm{d}a_t$ using Eq. 24. Also, calculate the increment of gel barrier $\mathrm{d}z_t$ using Eq. 25 and Eq. 28. In addition, using these increments calculate the updated values for α_t, a_t and z_t.
9. Finally calculate the increment of relative humidity $\mathrm{d}h_t^p$, saturation degree $\mathrm{d}S_t^{ip}$ and inter-particle porosity $\mathrm{d}\phi_t^{ip}$ using Eqs. 30, 31 and 32. Also, using these increments calculate the updated humidity, saturation degree and inter-particle porosity. For sake of simplicity the desorption isotherm slope may be calculated as $K_h = 1.2 - w/c$ (if the aim is calculating shrinkage, the more complex function for desorption isotherm should be considered; look at the model by Di Luzio and Cusatis [47]).

9. Conclusions

1. Long-term cement hydration advancing over decades or even a century can be explained by the proposed new model in which the hydration rate is controlled by diffusion of water from capillary pores through gradually thickening barrier shells of C-S-H that envelop gradually consumed remnants of cement grains.
2. A simple formulation can be obtained by assuming the cross-barrier diffusion to be controlled by a difference in humidity across the barrier, equivalent to the difference in chemical potential of water, while the hydration reaction at the interface of anhydrous cement with the C-S-H barrier is considered virtually immediate.

3. Although, during the first 4 to 24 hours, the C-S-H forms numerous discontinuous nano-globules around the cement grains, a simple model can be obtained by introducing and calibrating an equivalent barrier shell control of the hydration rate.
4. After calibration of the proposed model by published data, good agreement is achieved with the measured evolution of hydration degree and hydration heat for various cement types, particle size distributions, water-cement ratios and temperatures.
5. The decades-long continuation of cement hydration appears to be a hypothesis that can explain why the autogenous shrinkage of sealed specimens as well as the swelling in water immersion are recently observed to continue logarithmically for at least a decade.
6. Computationally, the model is sufficiently effective for being used as a subroutine for calculating the evolution of hydration degree or aging at every integration point of every finite element in a large structure.

Acknowledgment: Partial financial supports from the U.S. Department of Transportation, provided through Grant 20778 from the Infrastructure Technology Institute of Northwestern University, and from the NSF under grant CMMI-1129449, are gratefully appreciated.

10. References

[1] Z. P. Bažant, G.-H. Li, Comprehensive database on concrete creep and shrinkage, ACI Materials Journal 105 (6) (2008) 635–637. 1

[2] M. H. Hubler, R. Wendner, Z. P. Bažant, Comprehensive database for concrete creep and shrinkage: Analysis and recommendations for testing and recording, ACI (accepted). 1

[3] Z. P. Bažant, M. H. Hubler, Q. Yu, Excessive creep deflections: An awakening, Concrete International 33 (8) (2011) 44–46. 1

[4] Bažant, Zdenek P and Yu, Qiang and Li, Guang-Hua, Excessive long-time deflections of prestressed box girders. I: Record-span bridge in palau and other paradigms, Journal of Structural Engineering 138 (6) (2012) 676–686. 1

[5] Z. Bažant, M. Hubler, R. Wendner, Model B4 for creep, drying shrinkage and autogenous shrinkage of normal and high-strength concretes with multi-decade applicability, TC-242-MDC multi–decade creep and shrinkage of concrete: material model and structural analysis. RILEM Mater. Struct. 1

[6] R. Wendner, M. H. Hubler, Z. P. Bažant, Statistical justification of model B4 for multi-decade concrete creep using laboratory and bridge databases and comparisons to other models, Materials and Structures 48 (4) (2015) 815–833. 1

[7] Z. Bažant, A. Donmez, E. Masoero, S. R. Aghdam, Interaction of concrete creep, shrinkage and swelling with water, hydration, and damage: Nano-Macro-Chemo, in: 10th International Conference on Mechanics and Physics of Creep, Shrinkage, and Durability of Concrete and Concrete Structures, 2015. 1, 1

[8] H. M. Jennings, S. K. Johnson, Simulation of microstructure development during the hydration of a cement compound, Journal of the American Ceramic Society 69 (11) (1986) 790–795. 1

[9] D. P. Bentz, E. J. Garboczi, Digitized simulation model for microstructural development, Ceramic Transactions, 16 pp. 211. 1

[10] K. Van Breugel, Simulation of hydration and formation of structure in hardening cement-based materials, TU Delft, Delft University of Technology, 1991. 1

[11] P. Navi, C. Pignat, Simulation of cement hydration and the connectivity of the capillary pore space, Advanced Cement Based Materials 4 (2) (1996) 58–67. 1

[12] D. P. Bentz, Three-dimensional computer simulation of Portland cement hydration and microstructure development, Journal of the American Ceramic Society 80 (1) (1997) 3–21. 1

[13] K. Maekawa, R. Chaube, T. Kishi, Modeling of concrete performance: hydration, microstructure formation and mass transport, E and FN SPON, London. 1

[14] F. Lin, C. Meyer, Hydration kinetics modeling of Portland cement considering the effects of curing temperature and applied pressure, Cement and Concrete Research 39 (4) (2009) 255–265. 1, 6

[15] Z. P. Bažant, M. Jirásek, M. Hubler, I. Carol, RILEM draft recommendation: TC-242-MDC multi-decade creep and shrinkage of concrete: material model and structural analysis. model B4 for creep, drying shrinkage and autogenous shrinkage of normal and high-strength concretes with multi-decade applicability, Materials and structures 48 (4) (2015) 753–770. 1

[16] Z. P. Bažant, A. B. Hauggaard, S. Baweja, F.-J. Ulm, Microprestress-solidification theory for concrete creep. I: Aging and drying effects, Journal of Engineering Mechanics 123 (11) (1997) 1188–1194. 1

[17] Z. P. Bažant, X. Yunping, Drying creep of concrete: constitutive model and new experiments separating its mechanisms, Materials and Structures 27 (1) (1994) 3–14. 1

[18] B. Persson, Self-desiccation and its importance in concrete technology., Nordic Concrete Research. 21 (1998) 120–129. 1

[19] R. J. Flatt, G. W. Scherer, J. W. Bullard, Why alite stops hydrating below 80% relative humidity, Cement and Concrete Research 41 (9) (2011) 987–992. 1

[20] Z. Bažant, L. Najjar, Nonlinear water diffusion in nonsaturated concrete, Matériaux et Construction 5 (1) (1972) 3–20. 1, 4, 6

[21] H. F. Taylor, Cement chemistry, Thomas Telford, 1997. 2

[22] F.-J. Ulm, G. Constantinides, F. Heukamp, Is concrete a poromechanics materials?a multiscale investigation of poroelastic properties, Materials and structures 37 (1) (2004) 43–58. 2, 2, 6

[23] M. J. A. Qomi, F.-J. Ulm, R. J.-M. Pellenq, Physical origins of thermal properties of cement paste, Physical Review Applied 3 (6) (2015) 064010. 2

[24] M. J. A. Qomi, M. Bauchy, F.-J. Ulm, R. J.-M. Pellenq, Anomalous composition-dependent dynamics of nanoconfined water in the interlayer of disordered calcium-silicates, The Journal of Chemical Physics 140 (5) (2014) 054515. 2

[25] M. Königsberger, C. Hellmich, B. Pichler, Densification of csh is mainly driven by available precipitation space, as quantified through an analytical cement hydration model based on nmr data, Cement and Concrete Research 88 (2016) 170–183. 2, 6

[26] A. C. Muller, K. L. Scrivener, A. M. Gajewicz, P. J. McDonald, Densification of c–s–h measured by 1h nmr relaxometry, The Journal of Physical Chemistry C 117 (1) (2012) 403–412. 2, 6

[27] V. Baroghel-Bouny, M. Mainguy, T. Lassabatere, O. Coussy, Characterization and identification of equilibrium and transfer moisture properties for ordinary and high-performance cementitious materials, Cement and Concrete Research 29 (8) (1999) 1225–1238. 3

[28] J. W. Bullard, H. M. Jennings, R. A. Livingston, A. Nonat, G. W. Scherer, J. S. Schweitzer, K. L. Scrivener, J. J. Thomas, Mechanisms of cement hydration, Cement and Concrete Research 41 (12) (2011) 1208–1223. 4, 4

[29] H. Stein, J. Stevels, Influence of silica on the hydration of 3 CaO, SiO2, Journal of Applied Chemistry 14 (8) (1964) 338–346. 4

[30] H. Jennings, P. Pratt, An experimental argument for the existence of a protective membrane surrounding Portland cement during the induction period, Cement and Concrete Research 9 (4) (1979) 501–506. 4

[31] H. M. JENNINGS, Aqueous solubility relationships for two types of calcium silicate hydrate, Journal of the American Ceramic Society 69 (8) (1986) 614–618. 4

[32] E. M. Gartner, J. M. Gaidis, Hydration mechanisms: I, Materials Science of Concrete III, I, 1 pp. 95. 4

[33] J. W. Bullard, A determination of hydration mechanisms for tricalcium silicate using a kinetic cellular automaton model, Journal of the American Ceramic Society 91 (7) (2008) 2088–2097. 4

[34] P. Barret, D. Ménétrier, Filter dissolution of C3S as a function of the lime concentration in a limited amount of lime water, Cement and Concrete Research 10 (4) (1980) 521–534. 4

[35] P. Barret, D. Ménétrier, D. Bertrandie, Mechanism of C3S dissolution and problem of the congruency in the very initial period and later on, Cement and Concrete Research 13 (5) (1983) 728–738. 4

[36] S. Garrault, A. Nonat, Hydrated layer formation on tricalcium and dicalcium silicate surfaces: experimental study and numerical simulations, Langmuir 17 (26) (2001) 8131–8138. 4

[37] D. Damidot, F. Bellmann, B. Möser, T. Sovoidnich, Calculation of the dissolution rate of tricalcium silicate in several electrolyte compositions, Cement Wapno Beton 12 (74) (2007) 2. 4

[38] S. Garrault-Gauffinet, A. Nonat, Experimental investigation of calcium silicate hydrate (CSH) nucleation, Journal of Crystal Growth 200 (3) (1999) 565–574. 4

[39] T. Powers, T. Brownyard, Studies of the physical properties of hardened Portland cement paste, Bulletin 22. 4, 6

[40] P. Halamickova, R. J. Detwiler, D. P. Bentz, E. J. Garboczi, Water permeability and chloride ion diffusion in Portland cement mortars: relationship to sand content and critical pore diameter, Cement and Concrete Research 25 (4) (1995) 790–802. 4

[41] J. W. Bullard, G. W. Scherer, J. J. Thomas, Time dependent driving forces and the kinetics of tricalcium silicate hydration, Cement and Concrete Research 74 (2015) 26–34. 5

[42] M. M. C. Fernandez, Effect of particle size on the hydration kinetics and microstructural development of tricalcium silicate, Ph.D. thesis, EPFL (2008). 5, 8

[43] U. Danielson, Heat of hydration of cement as affected by water-cement ratio, in: Paper IV-S7, proceedings of the 4th international symposium on the chemistry of cement, Washington DC, USA, 1962, pp. 519–26. 6, 6

[44] D. P. Bentz, Influence of water-to-cement ratio on hydration kinetics: simple models based on spatial considerations, Cement and Concrete Research 36 (2) (2006) 238–244. 6, 6

[45] W. Lerch, C. Ford, Long-time study of cement performance in concrete, in: Journal Proceedings, Vol. 44, 1948, pp. 745–796. 7

[46] Z. Jiang, Z. Sun, P. Wang, Internal relative humidity distribution in high-performance cement paste due to moisture diffusion and self-desiccation, Cement and Concrete Research 36 (2) (2006) 320–325. 7

[47] G. Di Luzio, G. Cusatis, Hygro-thermo-chemical modeling of high performance concrete. i: Theory, Cement and Concrete composites 31 (5) (2009) 301–308. 9